

# Identification of Low Intratumoral Gene Expression Heterogeneity in Neuroblastic Tumors by Genome-Wide Expression Analysis and Game Theory

Domenico Albino, MS<sup>1</sup>  
 Paola Scaruffi, PhD<sup>2</sup>  
 Stefano Moretti, PhD<sup>3</sup>  
 Simona Coco, PhD<sup>2</sup>  
 Mauro Truini, MD<sup>4</sup>  
 Claudio Di Cristofano, MD<sup>5</sup>  
 Andrea Cavazzana, MD<sup>6</sup>  
 Sara Stigliani, PhD<sup>2</sup>  
 Stefano Bonassi, PhD<sup>7</sup>  
 Gian Paolo Tonini, PhD<sup>2</sup>

<sup>1</sup> Laboratory of Italian Neuroblastoma Foundation, National Cancer Research Institute, Genoa, Italy.

<sup>2</sup> Translational Pediatric Oncology, National Cancer Research Institute, Genoa, Italy.

<sup>3</sup> Epidemiology and Biostatistics, National Cancer Research Institute, Genoa, Italy.

<sup>4</sup> Department of Pathology, National Cancer Research Institute, Genoa, Italy.

<sup>5</sup> Department of Experimental Medicine, Sapienza University of Rome, Latina, Italy.

<sup>6</sup> Unit of Surgical Pathology, Department of Oncology, Azienda Sanitaria Locale n. 1, Carrara, Italy.

<sup>7</sup> Molecular Epidemiology, National Cancer Research Institute, Genoa, Italy.

The work was supported by: Fondazione Italiana per la Lotta al Neuroblastoma, Associazione Italiana per la Ricerca sul Cancro (AIRC), Ministero dell'Università e Ricerca Scientifica, Ministero della Salute, EU project NewGeneris, EU 6FP (FOOD-CT-2005-016320). D.A. is a fellow of the Italian Neuroblastoma Foundation.

The authors declare no conflict of interest.

The first two authors contributed equally to this article.

**BACKGROUND.** Neuroblastic tumors (NTs) are largely comprised of neuroblastic (Nb) cells with various quantities of Schwannian stromal (SS) cells. NTs show a variable genetic heterogeneity. NT gene expression profiles reported so far have not taken into account the cellular components. The authors reported the genome-wide expression analysis of whole tumors and microdissected Nb and SS cells.

**METHODS.** The authors analyzed gene expression profiles of 10 stroma-poor NTs (NTs-SP) and 9 stroma-rich NTs (NTs-SR) by microarray technology. Nb and SS cells were isolated by laser microdissection from NTs-SP and NTs-SR and probed with microarrays. Gene expression data were analyzed by the Significance Analysis of Microarrays (SAM) and Game Theory (GT) methods, the latter applied for the first time to microarray data evaluation.

**RESULTS.** SAM identified 84 genes differentially expressed between NTs-SP and NTs-SR, whereas 50 were found by GT. NTs-SP mainly express genes associated with cell replication, nervous system development, and antiapoptotic pathways, whereas NTs-SR express genes of cell-cell communication and apoptosis. Combining SAM and GT, the authors found 16 common genes driving the separation between NTs-SP and NTs-SR. Five genes overexpressed in NTs-SP encode for nuclear proteins (*CENPE*, *EYAL1*, *PBK*, *TOP2A*, *TFAP2B*), whereas only 1 of 11 highly expressed genes in NTs-SR encodes for a nuclear receptor (*NR4A2*).

**CONCLUSIONS.** The results showed that NT-SP and NT-SR gene signatures differ for a set of genes involved in distinct pathways, and the authors demonstrated a low intratumoral heterogeneity at the mRNA level in both NTs-SP and NTs-SR. The combination of SAM and GT methods may help to better identify gene expression profiling in NTs. *Cancer* 2008;113:1412-22. © 2008 American Cancer Society.

**KEYWORDS:** neuroblastic tumors, Schwannian cells, microarray, laser capture microdissection, Game Theory.

**T**umor tissue heterogeneity is a well-known feature of solid tumors. Neuroblastic tumors (NTs) are pediatric cancers composed of neuroblastic (Nb) and various amounts of Schwannian

We are grateful to Dr. C. Gambini (G. Gaslini Institute, Genoa, Italy) for providing tumor specimens; Dr. S. Salvi (National Cancer Research Institute, Genoa, Italy) for immunohistochemistry analysis; Dr. S. Cohn (University of Chicago, Chicago, Illinois), Dr. A. Bellacosa (Fox Chase Cancer Center, Philadelphia, Pennsylvania), and Dr. U. Pfeffer (National Cancer Research Institute, Genoa, Italy) for comments and suggestions.

Address for reprints: Gian Paolo Tonini, PhD, Translational Pediatric Oncology, National Cancer Research Institute (IST), Largo R. Benzi, 10, 16132 Genoa, Italy; Fax: (011) 39-010-5737487; E-mail: gianpaolo.tonini@istge.it

Received November 2, 2007; revision received March 4, 2008; accepted April 21, 2008.

stromal (SS) cells. Most NTs have sheets of malignant undifferentiating, poorly differentiated, or differentiated Nb cells, with very few or absent SS cells. These tumors are grouped as neuroblastoma (Schwannian stroma-poor). Smaller subsets of NTs, characterized by abundant SS cells, are classified as ganglioneuroblastoma (Schwannian stroma-rich) intermixed or nodular and ganglioneuroma.<sup>1</sup> Although genotype-phenotype association has been investigated by genome-wide transcriptome analysis,<sup>2-6</sup> the broad range of neuroblast differentiation and the variable stroma content in NTs make it difficult to assess cell-type specific signatures.

We previously reported that stroma-rich NTs (NTs-SR) have a lower degree of genetic instability than stroma-poor NTs (NTs-SP).<sup>7</sup> Furthermore, unsupervised analysis highlighted 2 gene clusters that drive the separation between NTs-SP and NTs-SR.<sup>7</sup> In the present study, we analyzed gene expression profiles of NTs-SP and NTs-SR using approaches based on Significance Analysis of Microarrays (SAM)<sup>8</sup> and Game Theory (GT).<sup>9-11</sup> Eighty-four and 50 genes were found differentially expressed by SAM and GT, respectively. GT offers the advantage of selecting relevant genes according to interactions among genes and not only their expression profile. Moreover, it takes into account that some genes may act as intermediate steps in a regulatory pathway.<sup>12</sup> Combining SAM and GT, we found 16 genes differentially expressed between NTs-SP and NTs-SR. In addition, we analyzed gene expression of microdissected Nb and SS cells, and observed low intratumoral heterogeneity at the mRNA level in both NTs-SP and NTs-SR.

## MATERIALS AND METHODS

### Patients and Tumor Samples

Nineteen primary tumor samples (10 NTs-SP and 9 NTs-SR) were collected at the onset of disease. The study was approved by the institutional ethical committees, and informed consent was obtained for each patient. Patients were staged according to the International Neuroblastoma Staging System<sup>13</sup> as follows: stage 1, 10; stage 2A, 2; stage 3, 2; stage 4, 4; and stage 4S, 1. Tumors were classified according to the International Neuroblastoma Pathology Committee.<sup>1</sup> NT-SP samples had at least 90% Nb cells, and the NTs-SR had SS cells ranging from 80% to 90%.

### Gravity-assisted Laser Microdissection

Laser capture microdissection (LCM) was performed on 2 NT-SP (#1919, #2182) and 2 NT-SR (#1589, #1761) frozen specimens. Approximately 800 to 3000 cells were collected from each tissue area. Sections

of 4  $\mu\text{m}$  were cut using a cryostat and mounted onto PEN Membrane Slides (Leica Microsystems, Bannockburn, Ill) according to the manufacturer's recommendations. Different areas from each tumor were collected and separately analyzed. Serial sections were cut for each sample: the first was stained with hematoxylin and eosin for cell content evaluation; subsequent slides were lightly stained with Mayer hematoxylin and used for LCM. On the basis of cellular composition, selected areas were microdissected and immediately collected in a tube containing PicoPure RNase-inhibitor solution (Arcturus Engineering, Mountain View, Calif). The entire procedure was quickly performed at room temperature.

### RNA Purification

Total RNA was extracted from bulk tumors and from LCM-derived specimens by using the Perfect RNA Eukaryotic Mini Kit (Eppendorf, Hamburg, Germany) and the PicoPure RNA isolation kit (Arcturus Engineering), respectively. RNA was checked with a 2100 BioAnalyzer instrument (Agilent Technologies GmbH, Waldbronn, Germany), and only RNA samples with RNA integrity number  $\geq 7$  were included in the study.

### Microarray Experiments for Gene Expression Analysis

Gene expression analysis was performed by using Human Genome U133A GeneChip arrays (Affymetrix, Inc., Calif) as previously described.<sup>7</sup> Experimental and analytical processes were performed according to the MIAME checklist ([www.mged.org/index.html](http://www.mged.org/index.html)). The number of independent biological samples necessary for testing whether genes are differentially expressed between NTs-SP and NTs-SR has been calculated considering the number of comparisons among the gene sequences ( $n = 22,283$ ) present on the microarray. We assumed that genes are independent and that a false-positive rate of  $\alpha = 0.001$  gives no more than 23 expected false-positives. We established that a two-fold difference of mean expression levels between NTs-SP and NTs-SR was a meaningful value to identify a differential expression. Furthermore, we fixed that standard deviation (SD) of  $\log_2$  signals among tumor samples of Affymetrix GeneChip<sup>TM</sup> is  $\sigma = 0.5$  according to Simon et al.<sup>14</sup> Finally, we set a false negative rate of  $\beta = 0.2$ . According to these parameters the required sample size of each group was 9.<sup>14</sup>

### Data Processing

Microarray data were pre-processed by "Affy" software package<sup>15</sup> (Affymetrix). No background correc-

tion was performed and probe intensities were normalized using the *vsn*<sup>16</sup> method. Expression measures were computed by the medianpolish method and only perfect match probes were accepted and used in the algorithm.<sup>17</sup> Within this framework, each hybridization experiment produced an array of expression values corresponding to  $n = 22,283$  gene sequences. Data from a series of  $m$  experiments was represented as a gene expression matrix  $\mathbf{X}$ , with  $n$  rows and  $m$  columns, where the  $i$ th row consists of an  $m$ -element expression vector  $\mathbf{X}_i = (X_{i1}, \dots, X_{im})$  for a single gene sequence. Since we compared the expression profiles of two conditions, namely the tumor categories NTs-SP and NTs-SR, with 10 NT-SP and 9 NT-SR biological replicates, respectively, data set was split in two expression matrix:  $\mathbf{X}^{SP}$  and  $\mathbf{X}^{SR}$ .

**Significance Analysis of Microarrays**

For each gene sequence  $i$ , SAM computed an observed score  $d_{(i)}$ , which is a modified t-statistic as described by Storey and Tibshirani.<sup>18</sup> The index, based on the SD of repeated measurements under two conditions, assesses the difference of gene expression average between the two conditions. The observed score  $d_{(i)}$  was compared to the distribution of expected score  $\hat{d}_{(i)}$  estimated by random permutations of repeated measurements. This comparison was used to estimate the proportion of false positives among genes called significant, i.e., the *false discovery rate* (FDR).<sup>18-20</sup> For a fixed threshold  $\Delta$ , each gene  $i$ , with an absolute score difference  $|d_{(i)} - \hat{d}_{(i)}| \geq \Delta$ , was called significant according to SAM as modified by Storey and Tibshirani.<sup>18</sup> We applied SAM to expression matrices  $\mathbf{X}^{SP}$  and  $\mathbf{X}^{SR}$  to identify gene sequences with significant changes in expression levels between NTs-SP and NTs-SR. The analysis was performed using the R package “siggenes” (www.r-project.org).

**Game Theory Method**

A *Coalitional game*<sup>9</sup> is a pair  $(N, v)$ , where  $N$  denotes a finite set of players and  $v: 2^N \rightarrow IR$  the *characteristic function*, with  $v(\emptyset) = 0$ . A group of players  $T \subseteq N$  is called a *coalition* and the real value  $v(T)$  is the worth of coalition  $T$ . A *solution* for a class of coalitional games is a function  $\psi$  that assigns a vector number  $\psi(v) \in IR^N$  to each coalitional game in the class. A well-known solution for coalitional games is the *Shapley value*.<sup>10</sup> The Shapley value assigns to each player his *average marginal contribution* over all the possible orderings, i.e., permutations of players. Formally, given a coalitional game  $(N, v)$ , for each player  $i \in N$  the Shapley value  $\phi_i(v)$  is defined by

$$\phi_i(v) = \frac{1}{n!} \sum_{\pi} v(P(\pi, i) \cup \{i\}) - v(P(\pi, i)) \quad (1)$$

where  $\pi$  is a permutation of players;  $P(\pi, i)$  is the set of players that precedes player  $i$  in the permutation  $\pi$ , and  $n$  is the cardinality of  $N$ .

Let  $N = \{1, \dots, n\}$  be a set of genes. A microarray game is a coalitional game  $(N, w)$  where the function  $w$  assigns to each coalition  $S \subseteq N$  a frequency of associations, between a *condition* and a *expression property*, of genes realized in the coalition  $S$ . Different gene expression properties might be considered: eg, under- or over-expression and significant variation.<sup>11</sup> A key issue for the definition of a microarray game  $(N, w)$  is the notion of association between a *condition* and a *gene expression property* inside a coalition  $S \subseteq 2^N \setminus \{\emptyset\}$ . For *condition* we mean whatever state of the biological samples that possible affects gene expression (i.e. disease state, the exposure to environmental or therapeutic agents). On a single array, a sufficient requirement to realize the association between a *condition* and an *expression property* in a coalition  $S \subseteq N$  is that all genes showing such *expression property* belong to the coalition  $S$  (*sufficiency principle for groups of genes*). Coalition  $S$  is called a *winning coalition*.

We refer to a Boolean matrix  $\mathbf{B} \in \{0, 1\}^{n \times k}$ , where  $k \geq 1$  is the number of arrays, and where the Boolean values 0-1 represent two complementary expression properties, for example the normal expression (coded by 0) and the over-expression (coded by 1). Let  $\mathbf{B}_j$  be the  $j$ -th column of  $\mathbf{B}$ , we define the *support* of  $\mathbf{B}_j$ , denoted by  $sp(\mathbf{B}_j)$ , as the set  $sp(\mathbf{B}_j) = \{i \in \{1, \dots, n\} \text{ such that } \mathbf{B}_{ij} = 1\}$ . The microarray game corresponding to  $\mathbf{B}$  as the coalitional game  $(N, w)$ , where  $w: 2^N \rightarrow IR^+$  is such that  $w(T)$  is the rate of occurrences of coalition  $T$  as a winning coalition, i.e. as a superset of the supports in the Boolean matrix  $\mathbf{B}$ ; in formula, we define  $w(T)$ , for each  $T \in 2^N \setminus \{\emptyset\}$ , as the value

$$w(T) = \frac{c(\Theta(T))}{k} \quad (2)$$

where  $c(\Theta(T))$  is the cardinality of the set  $\Theta(T) = \{j \in K \text{ such that } sp(\mathbf{B}_j) \subseteq T, sp(\mathbf{B}_j) \neq \emptyset\}$ , with  $K = \{1, \dots, k\}$  and  $v(\emptyset) = 0$ . Since it is computationally too expensive to calculate the Shapley value  $\phi(w)$  of game  $(N, w)$  according to the relation (1), Moretti et al.<sup>11</sup> introduced an easy way to calculate  $\phi(w)$  for whatever microarray game  $(N, w)$ .

**Game Theory Analysis**

The first step of GT analysis considered the “gene expression property encoding”, a procedure aimed to discriminate over-regulated genes in both NTs-SP

and NTs-SR. Each continuous value in the vector  $X_i^{SP} = (X_{i1}^{SP}, \dots, X_{i10}^{SP})$  (or  $X_i^{SR} = (X_{i1}^{SR}, \dots, X_{i9}^{SR})$ ), which was  $\geq 1.5 \times \text{MEAN}[X_i^{SR}]$  (or  $\geq 1.5 \times \text{MEAN}[X_i^{SP}]$ ), was coded as 1, or 0 if otherwise. Consequently, a Boolean matrix  $B^{SP}$  with  $n$  rows and 10 columns with values  $\{0,1\}$  was generated from  $X^{SP}$ , and analogously, a Boolean matrix  $B^{SR}$  with  $n$  rows and 9 columns with values  $\{0,1\}$  was generated from  $X^{SR}$ . From both Boolean matrices  $B^{SP}$  and  $B^{SR}$ , two microarray games<sup>11</sup>  $(N, w^{SP})$  and  $(N, w^{SR})$  were computed, respectively, according to relation (2). To evaluate for each gene the strength of the association between the expression property and the conditions (NTs-SP and NTs-SR), we used the *Shapley value*<sup>10,11</sup> of games  $(N, w^{SP})$  and  $(N, w^{SR})$ . Genes showing the absolute difference of Shapley value  $\Delta\phi_i = |\phi_i(w^{SP}) - \phi_i(w^{SR})|$  greater than a predefined cutoff were selected for further analysis.

### Hierarchical Cluster Analysis and Gene Ontology

We used clustering analysis to detect similarities between NTs-SP and NTs-SR groups and between different tissue areas within the same tumor. All agglomerative hierarchical clusters were computed using the Euclidean distance between single vectors and the average linkage method. Heat-maps were representative of gene expression levels. All statistics were produced with the software R ([www.r-project.org](http://www.r-project.org)). Gene pathway analysis was performed with the NetAffy Gene Ontology Mining Tool ([www.affymetrix.com/analysis/index.affx](http://www.affymetrix.com/analysis/index.affx)).

### Quantitative Analysis of Gene Signatures by Real-Time Reverse Transcriptase Polymerase Chain Reaction

We performed real-time polymerase chain reaction (PCR) to validate all genes found differently expressed by SAM and GT. The TaqMan Low Density Array tool and 7900HT Fast Real-Time PCR System (Applied Biosystems, Foster City, Calif) were used according to the manufacturer's protocol. The 18S rRNA TaqMan probe (Applied Biosystems) was the internal control. Experiments were performed in triplicate. Cycle threshold ( $C_t$ ) was assigned at the initial logarithmic phase of PCR amplification and the difference between  $C_t$  values of each target gene ( $i$ ) and the control gene ( $\Delta C_t$ ) was used to normalize gene expression. Relative expression of each gene in NTs-SP was determined using the following formula:  $\Delta\Delta C_t(i) = \text{average}_{NTs-SP}[\Delta C_t(i)] - \text{average}_{NTs-SR}[\Delta C_t(i)]$ .

### Protein Isolation and Western Blot Analysis

Five available NT-SP and 5 NT-SR specimens were lysed with Mammalian cell extraction kit (MBL, Woburn, Mass), and protein content was measured

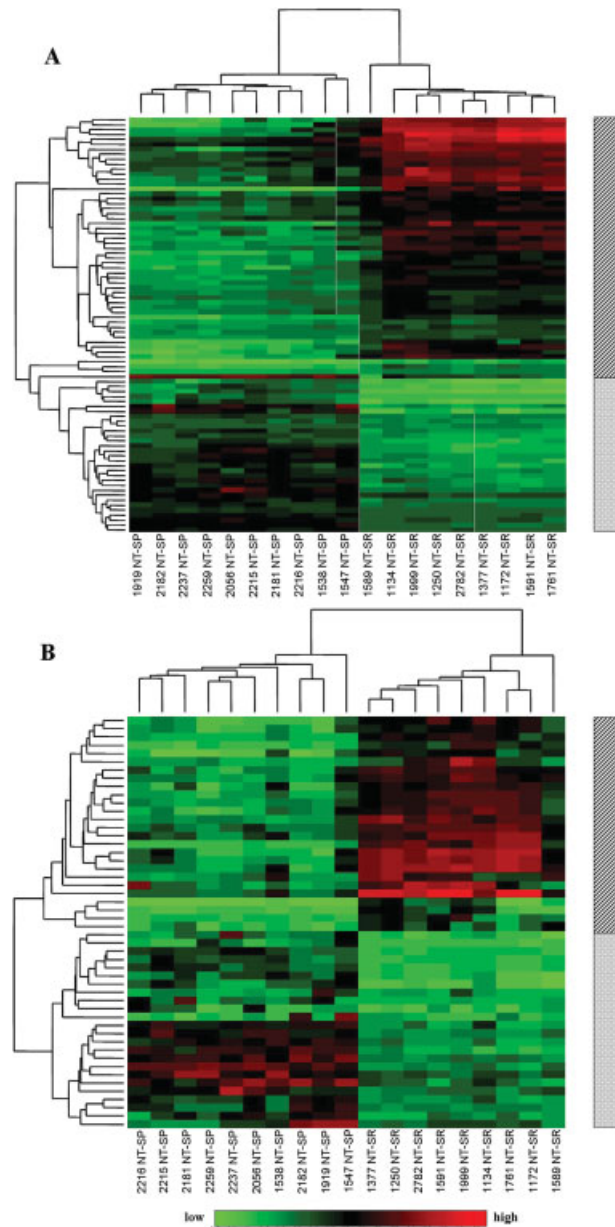


**FIGURE 1.** Hierarchical clustering dendrograms of 84 genes identified by SAM (A) and 50 genes identified by GT (B) in 10 stroma-poor neuroblastic tumors (NTs-SP) and 9 stroma-rich neuroblastic tumors (NTs-SR) are shown. Each color patch of the heat map represents the expression level of genes (row) in that tumor sample (column), with a continuum of expression levels from bright green (lowest) to bright red (highest). Dashed vertical bar indicates NT-SR gene signature; dotted bar, NT-SP gene signature; horizontal color bar, gene expression level.

using DC Protein assay (BioRad, Hercules, Calif). Fifty micrograms of each sample were resolved by sodium dodecyl sulfate polyacrylamide gel electrophoresis, transferred to nitrocellulose and saturated by Blocking agent (GE Healthcare, Buckinghamshire,

**TABLE 1**  
**Sixteen Genes Differentially Expressed in Stroma-Poor and Stroma-Rich Neuroblastic Tumors Selected by Both the Significance Analysis of Microarrays and Game Theory Methods**

No.	Gene Symbol	Accession Number*	Description	Biological Function
1	<i>ABCA8</i>	NM_007168	ATP-binding cassette, sub-family A (ABC1), member 8	Transport
2	<i>ANGPTL7</i>	NM_021146	Angiotensin-like 7	Response to oxidative stress
3	<i>APOD</i>	NM_001647	Apolipoprotein D	Lipid metabolism
4	<i>ASPA</i>	NM_000049	Aspartoacylase	Aminoacylase activity
5	<i>CYP1B1</i>	NM_000104	Cytochrome P450, family 1, subfamily B, polypeptide 1	Eye development
6	<i>GPM6B</i>	NM_001001994	Glycoprotein M6B	Cell differentiation
7	<i>MAL</i>	NM_002371	T-cell differentiation protein	Signal transduction
8	<i>NR4A2</i>	NM_001067	Nuclear receptor subfamily 4, group A, member 2	Transcription factor activity
9	<i>PLP1</i>	NM_000533	Proteolipid protein 1	Structural molecule activity
10	<i>PMP2</i>	NM_002677	Peripheral myelin protein 2	Transporter activity
11	<i>TSPAN8</i>	NM_004616	Tetraspanin 8	Protein amino acid glycosylation
12	<i>CENPF</i>	NM_016343	Centromere protein F (mitosin)	Cell cycle control
13	<i>EYA1</i>	NM_172058	Eyes absent homolog 1 ( <i>Drosophila</i> )	Regulation of transcription
14	<i>PBK</i>	NM_018492	PDZ-binding kinase	Cell cycle control
15	<i>TFAP2B</i>	NM_003221	Transcription factor AP-2 beta	Transcription factor activity
16	<i>TOP2A</i>	NM_001067	Topoisomerase (DNA) II alpha	Cell cycle control

Genes from 1 to 11 are more expressed in stroma-rich neuroblastic tumors; genes from 12 to 16 are more expressed in stroma-poor neuroblastic tumors.

\*Accession Number according to <http://ncbi.nlm.nih.gov/entrez>.

UK). Blots were incubated with the following antibodies: mouse monoclonal anti-TOP2A (Abnova, Taipei City, Taiwan), purified rabbit antihuman NR4A2 polyclonal antibody (Proteintech Group, Chicago, Ill), and anti-glyceraldehyde-3-phosphate dehydrogenase loading control (Abcam, Cambridge, UK) according to manufacturers' recommendations. After washing, each blot was incubated with appropriate horseradish peroxidase secondary antibodies (Santa Cruz Biotechnology, Santa Cruz, Calif), and the antigen-antibody complex was revealed by Enhanced Chemi-Luminescence (ECL) solution (GE Healthcare) and short exposure to ECL Hyperfilm (GE Healthcare).

### Immunohistochemistry Analysis

Immunohistochemistry (IHC) analysis was performed using polymeric complex technique and automated immunostainer Benchmark XT (Ventana, Tucson, Ariz). One representative NT-SP paraffin-embedded tumor, after deparaffinization and rehydration, was incubated with monoclonal TOP2A (Abnova) antibody, and immunophosphatase assay was performed. One representative NT-SR frozen sample, after antigen retrieval in 10 mM citric acid at pH 6.0, was incubated with polyclonal NR4A2 (Proteintech Group) antibody, and then immunoperoxidase staining was carried out. Primary antibodies were detected by UltraView™ Universal Dab and UltraViewRed™ detection kits (Ventana). Sections were counterstained with Gill modified hematoxylin (Ventana),

dehydrated, and mounted. Staining without primary antibody was performed as negative control.

## RESULTS

### NT-SP and NT-SR Signatures Identified by SAM

Microarray data are available at Gene Expression Omnibus (<http://www.ncbi.nlm.nih.gov/projects/geo/index.cgi>, accession number GSE7529). Eighty-four genes with an absolute score difference  $|d_{(i)} - \bar{d}_{(i)}| \geq \Delta = 6.09$  were selected by SAM (FDR = 0%). NTs-SP and NTs-SR are placed on different trunks of the hierarchical clustering dendrogram that separates NT categories according to their gene expression profiles (Fig. 1A). Fifty-two genes are more expressed in NTs-SR than in NTs-SP. This cluster comprises genes involved in signal transduction (*RGL1*, *STARD13*, *TGFBR3*, *EDNRB*, *ITPR3*, *HBEGF*, *CENTD1*, *TRIM38*), cell differentiation (*GPM6B*, *NDRG2*), and induction of apoptosis (*CLU*, *DUSP22*, *EGR3*, *FOXO1A*, *MAL*). The majority of 32 genes highly expressed in NTs-SP code for transcription factors (*NR4A2*, *EYA1*, *MCM4*, *EZH2*, *MLF11P*, *SOX4*, *PHOX2A*), proteins involved in the cell cycle (*ASPM*, *CENPE*, *LOC55565*, *SPAG5*, *GINS1*, *BUB1B*, *CXXC4*, *HIST3H2A*, *CDC25A*), nervous system development (*TFAP2B*, *DPYSL4*), and inhibition of apoptosis (*BIRC5*, *FEV*, *IL7*, *TMEM132A*).

### NT-SP and NT-SR Signatures Identified by GT

Fifty genes with an absolute Shapley difference  $\Delta\phi_i$  higher than  $MEAN(\Delta\phi_j)$  (data not shown) were

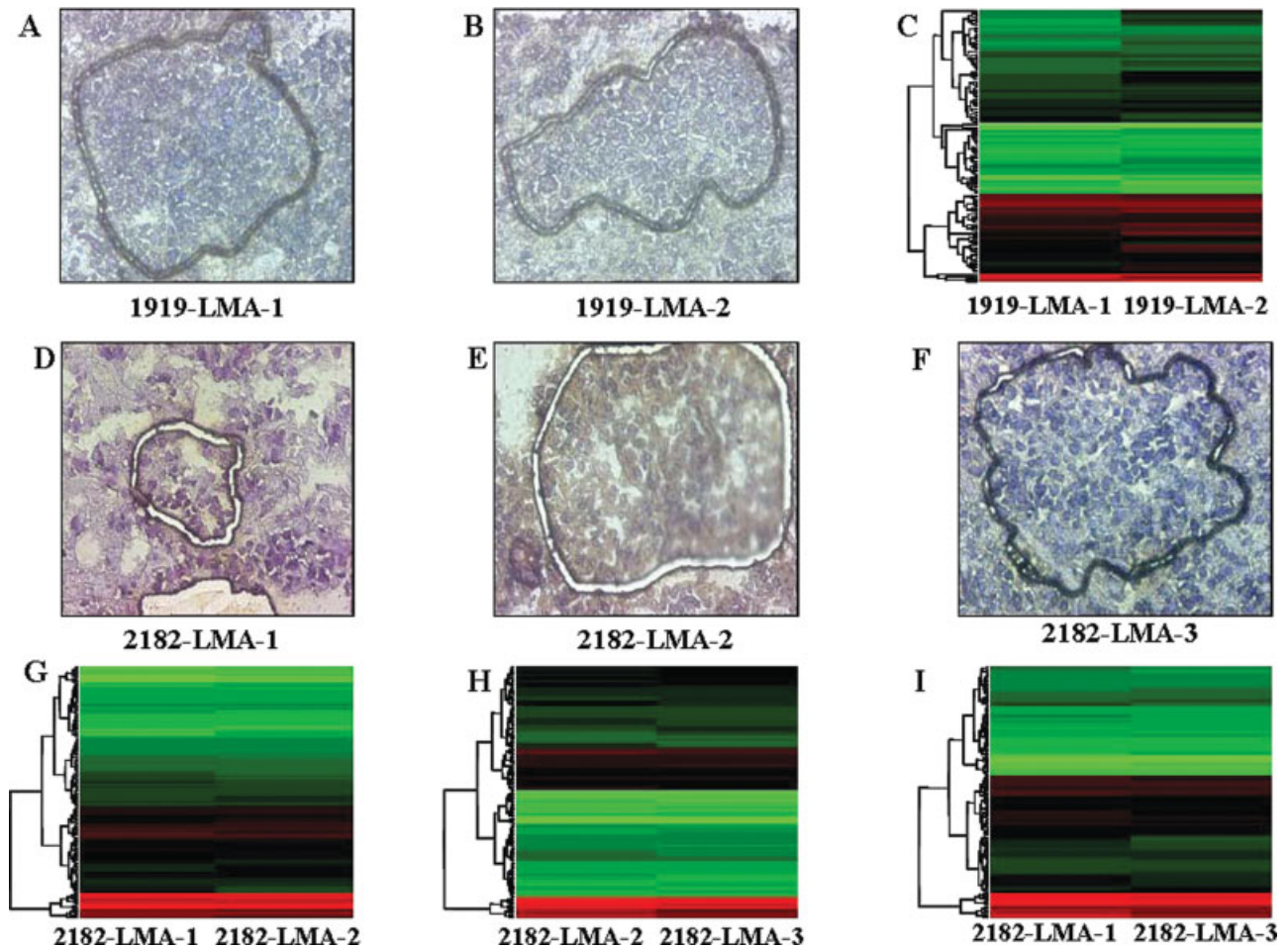


**FIGURE 2.** The upper panel shows gene expression analysis of microdissected cells from sample #1919, a stroma-poor neuroblastoma tumor. In each hematoxylin-stained cryosection, the line indicates the dissected areas, composed of round large neuroblastic (Nb) cells with large nuclei (A) and round small Nb cells with prominent nuclei (B) (magnification,  $\times 40$ ). The figure displays the hierarchical clustering dendrogram (C) of gene sequences identified by Significance Analysis of Microarrays (SAM) and Game Theory (GT). The Pearson correlation coefficient between gene expression profiles of 1919-Laser Microdissected Area (LMA)-1 and 1919-LMA-2 is  $r = 0.90$ ;  $P < .001$ . The lower panel shows gene expression analysis of microdissected cells from sample #2182, a stroma-poor neuroblastoma tumor. In each hematoxylin-stained cryosection, the line indicates the dissected areas, composed of round small Nb cells with large nuclei (D), round large Nb cells (E), and round large Nb cells with prominent nuclei (F) (magnification,  $\times 40$ ). The figure displays the hierarchical clustering dendrograms for the 2182-LMA-1 and 2182-LMA-2 areas (G), the 2182-LMA-2 and 2182-LMA-3 areas (H), and the 2182-LMA-1 and 2182-LMA-3 areas (I) of gene sequences selected by SAM and GT. The Pearson correlation coefficient between the 3 pairs of microdissected areas is  $r = 0.99$ ;  $P < .001$ .

selected by the GT method. NTs-SP and NTs-SR are placed on different trunks of the hierarchical clustering dendrogram (Fig. 1B), demonstrating that genes selected by GT successfully identify NTs-SP and NTs-SR according to their expression profile. Twenty-six genes are more expressed in NTs-SR than in NTs-SP. They include genes involved in signal transduction pathways (*GPR126*, *P2RY14*, *CHL1*, *CXCL13*, *CXCL14*), transcription regulation (*MEOX2*, *NR4A2*), cell differentiation (*CHL1*, *GPM6B*), and induction of apoptosis (*MAL*). Several genes up-regulated in NTs-SP are related to nervous system development (*TFAP2B*, *MAB21L2*, *POU4F2*), transcription regulation (*TNRC9*,

*GATA3*, *INSM1*, *TFAP2B*, *EYA1*, *MYCN*, *NHLH2*), cell cycle control (*CENPE*, *TTK*, *PBK*), and DNA repair (*TOP2A*, *RRM2*).

#### NT-SP and NT-SR Signatures Identified by Combined SAM and GT

Sixteen genes were identified as differentially expressed in NTs-SP and NTs-SR by both SAM and GT algorithms (Table 1). Eleven genes (*ABCA8*, *ANGPTL7*, *APOD*, *ASPA*, *CYP11B1*, *GPM6B*, *MAL*, *NR4A2*, *PLP1*, *PMP2*, *TSPAN8*) are highly expressed in NTs-SR, whereas 5 genes (*CENPE*, *EYA1*, *PBK*,

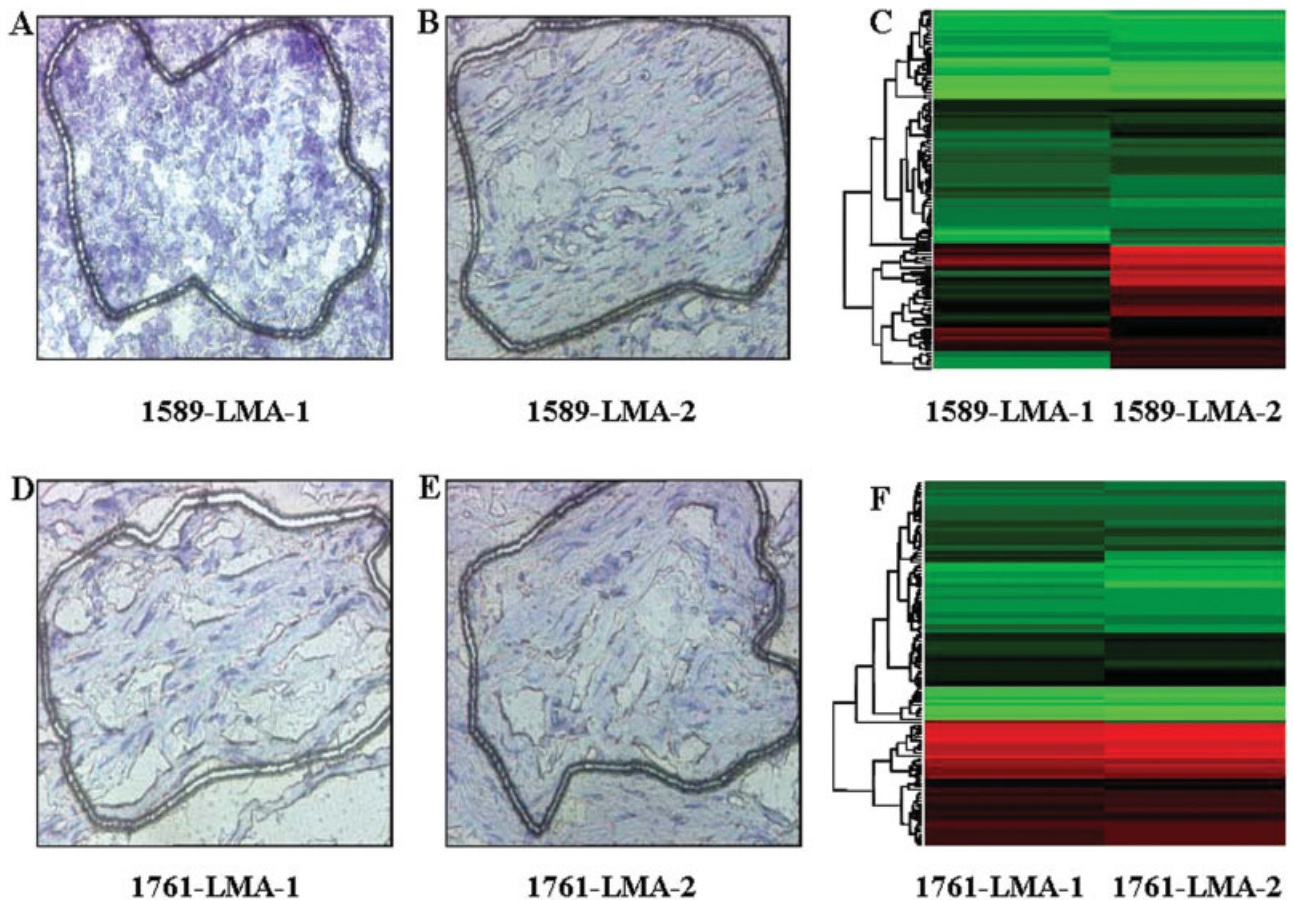


**FIGURE 3.** The upper panel shows gene expression analysis of microdissected cells from sample #1589, a stroma-rich neuroblastic tumor. In each hematoxylin-stained cryosection, the line indicates the dissected areas, composed of small round cells resembling neuroblasts embedded in Schwannian stromal (SS) cells (A) and SS cells with flat nuclei and elongated cytoplasm (B) (magnification,  $\times 40$ ). Panel C displays the hierarchical clustering dendrogram of gene sequences identified by Significance Analysis of Microarrays (SAM) and Game Theory (GT). The Pearson correlation coefficient between neuroblastic and SS microdissected areas is  $r = 0.76$ ;  $P < .001$ . The lower panel shows gene expression analysis of microdissected cells from sample #1761 NT-SR, a stroma-rich neuroblastic tumor. In each hematoxylin-stained cryosection, the line indicates 2 dissected areas composed of SS cells with flat nuclei and elongated cytoplasm (D and E). The figure displays the hierarchical clustering dendrogram (F) of gene sequences identified by SAM and GT. The Pearson correlation coefficient is  $r = 0.97$ ;  $P < .001$ . LMA indicates Laser Microdissected Area.

*TFAP2B*, *TOP2A*) are more highly expressed in NTs-SP than NTs-SR.

#### Microarray Data Validation

Quantitative real-time PCR confirmed results obtained by microarray technology, except in 5 genes (*ARHGAP15*, *CDC14B*, *RABGAP1L*, *SPTLC2*, *FYCO1*) that were thereby excluded from further analyses.

#### Gene Expression Profiling of Microdissected Nb and SS Cells

Two tissue areas were microdissected from sample #1919: 1919-Laser Microdissected Area (LMA)-1 (Fig. 2A), composed of large round Nb cells, and 1919-

LMA-2 (Fig. 2B), with small Nb cells. Small round undifferentiated Nb cells (2182-LMA-1, Fig. 2D) and large round Nb cells (2182-LMA-2 and 2182-LMA-3, Fig. 2E-2F) were isolated from sample #2182. Sample #1589 showed small round elements resembling Nb cells (1589-LMA-1, Fig. 3A) that were embedded within abundant SS cells (1589-LMA-2, Fig. 3B). Finally, 2 areas composed of homogeneous SS cells were microdissected from sample #1761: 1761-LMA-1 (Fig. 3D) and 1761-LMA-2 (Fig. 3E).

Hierarchical clustering analyses of 84 genes identified by SAM and 50 identified by GT grouped microdissected Nb and SS cells with bulk NTs-SP and NTs-SR, respectively (Fig. 4A and 4B). It is noteworthy that sample 1589-LMA-1, composed of

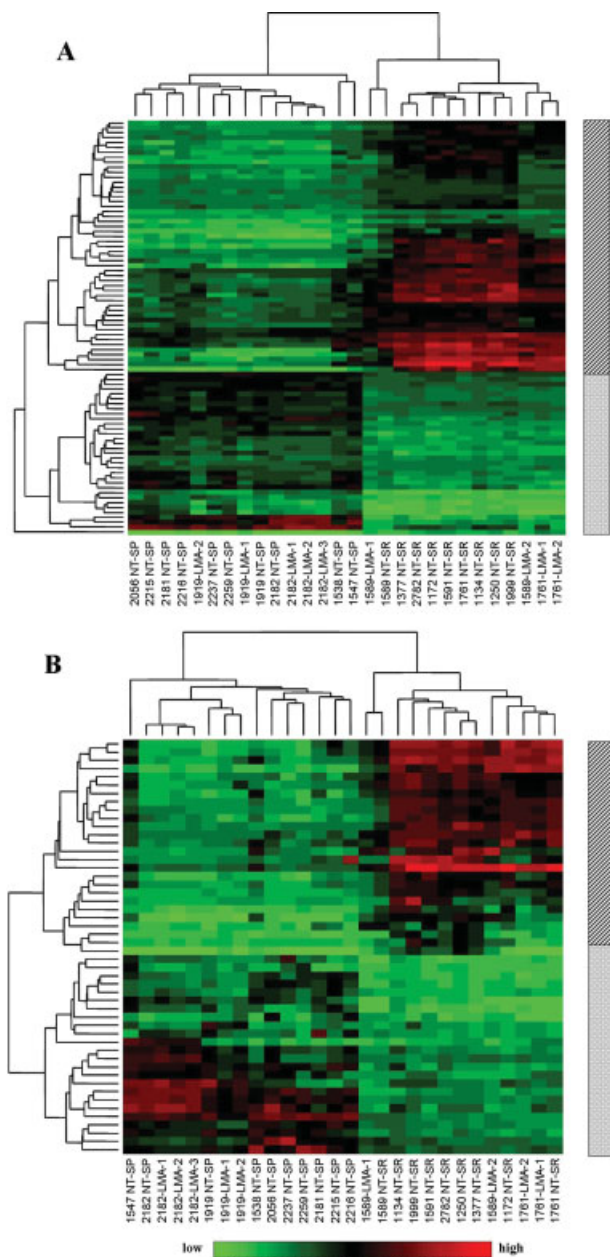


**FIGURE 4.** Hierarchical clustering dendrograms of 84 genes identified by Significance Analysis of Microarrays (SAM) (A) and 50 genes identified by Game Theory (GT) (B) in 10 stroma-poor neuroblastic tumors (NTs-SP), 9 stroma-rich neuroblastic tumors (NTs-SR), and 9 microdissected areas (5 areas containing neuroblastic [Nb] cells and 4 areas containing Schwannian stromal [SS] cells) are shown. Each color patch of the heat map represents the expression level of the associated gene (row) in the tumor sample (column), with a continuum of expression levels from bright green (lowest) to bright red (highest). Microdissected areas of SS and Nb cells fall into NT-SR and NT-SP categories, respectively. The dashed vertical bar indicates NTs-SR gene signature; dotted bar, NTs-SP gene signature; horizontal color bar, gene expression level.

neuroblasts embedded in stromal cells, falls in the NT-SR group.

Low heterogeneity of gene expression profiles within the same tumor was demonstrated by high Pearson correlation coefficients (0.90-0.99) for each pair of microdissected samples with similar cell morphology (Figs. 2C, 2G, 2H, 2I, 3C, and 3F). We found a lower correlation coefficient value ( $r = 0.76$ ) for microdissected Nb cells (1589-LMA-1) and their stromal counterpart (1589-LMA-2).

#### TOP2A and NR4A2 Protein Expression in NTs-SP and in NTs-SR

TOP2A and NR4A2 protein expression was evaluated in both NTs-SP and NTs-SR based on tumor sample availability. NTs-SP show a significant amount of TOP2A, and NTs-SR do not express the protein. Moreover, NR4A2 shows a higher expression in NTs-SR than in NTs-SP (Fig. 5A). This is in agreement with microarray results that show a differential level of gene expression between NTs-SR and NTs-SP. IHC analysis shows that TOP2A is expressed in Nb cells (Fig. 5B), and NR4A2 is localized in SS cells (Fig. 5C).

#### DISCUSSION

Because the relation between NTs' genotype and phenotype is largely unknown, we investigated genes differentially expressed between NTs-SP and NTs-SR by genome-wide transcriptome analysis. Eighty-four and 50 genes were differentially expressed in the 2 NT categories by using SAM and GT methods, respectively. Moreover, we assessed gene expression profiles of microdissected Nb and SS cells. As expected, Nb cells showed a "stroma-poor" signature, and SS cells showed a "stroma-rich" signature. Interestingly, when we compared gene expression profiles of Nb cells isolated from different areas within the same NT-SP sample, no significant differences were observed. Similarly, gene expression profiles of SS cells, microdissected from different areas of NTs-SR, were similar. We demonstrated a low intratumoral gene expression heterogeneity of NTs that does not reflect the genetic heterogeneity previously reported in neuroblastomas.<sup>7</sup> We think that DNA aberrations may be restricted to a few Nb clones of tumor cells without any effect on gene expression. We can also argue that nonrandom abnormalities at 1 or more loci in different clones is not significantly detected by microarray gene expression analysis. This matter should be taken into account in future studies aimed at comparing DNA imbalances and gene expression profiles of NTs.

It is noteworthy that in tumor #1589 the neuroblast nest (1589-LMA-1) embedded in Schwannian



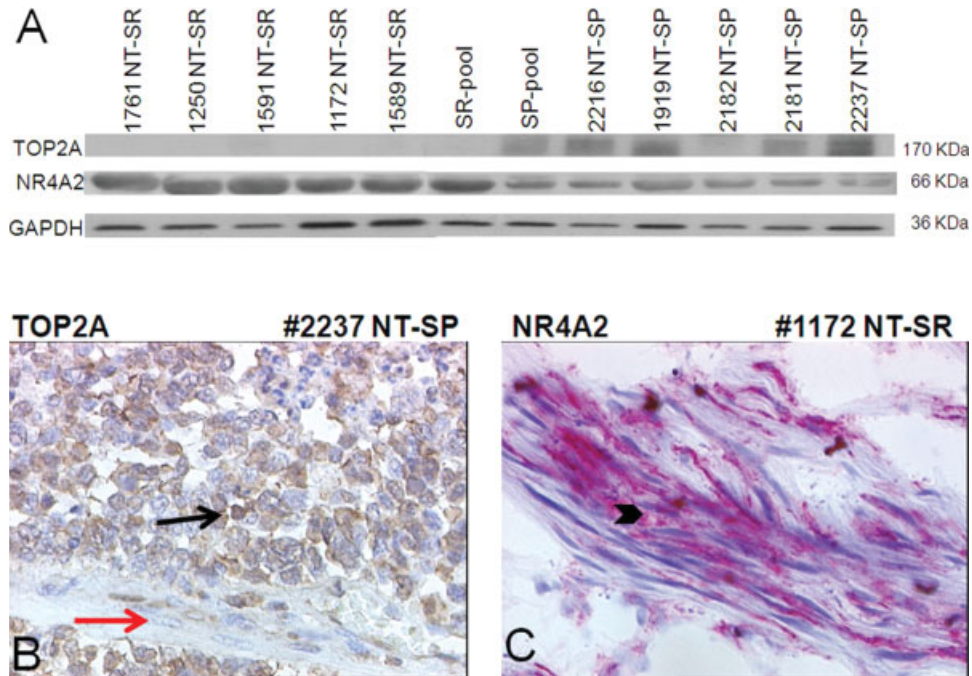


**FIGURE 5.** Western blot analysis of TOP2A and NR4A2 proteins is shown (A). The SP-pool consists of 10  $\mu$ g of each stroma-poor neuroblastic tumor (NT-SP) protein sample; the SR-pool consists of 10  $\mu$ g of each stroma-rich neuroblastic tumor (NT-SR) protein sample. TOP2A is expressed in 5 NTs-SP and the SP-pool, whereas it is undetectable in 5 NTs-SR and the SR-pool. NR4A2 expression is higher in 5 NTs-SR and the SR-pool than in 5 NTs-SP and the SP-pool. Immunohistochemistry analysis is shown of TOP2A (B) and NR4A2 proteins (C). TOP2A is prevalent in neuroblastic nuclei (black arrow) and absent in Schwannian stromal (SS) cells (red arrow). NR4A2 is localized in most of SS cell nuclei (black arrowhead) (magnification,  $\times 63$ ). GAPDH indicates glyceraldehyde-3-phosphate dehydrogenase.

stroma shows the NT-SR-associated signature. We postulate that surrounding SS cells may induce neuroblasts to acquire a Schwannian cell-like gene expression profile.

For the first time a GT-based procedure was used to analyze gene expression data and was combined with conventional SAM analysis. SAM selects genes according to their individual differential expression between NT-SP and NT-SR categories. The GT method offers the advantage of selecting relevant genes not only according to their expression level, but also taking into account interactions among genes. Thereby, we believe that combining SAM and GT approaches may be helpful to select those genes that play a key role in NT pathogenesis.

It is noteworthy that the *BIRC5* (survivin) gene, mapping at 17q25, has been found highly expressed in NTs-SP. *BIRC5* has been observed overexpressed in advanced neuroblastomas,<sup>2-4,21-24</sup> and Ito et al<sup>25</sup> showed that *BIRC5* up-regulation is associated with poor patient outcome. Thus, our results support the antiapoptotic role of *BIRC5* in NTs-SP and its malignant neuroblast-specific expression. NTs-SP express *CDC25A*, *TFAP2B*, and *MYCN* genes related to the

*p38-MAPK* pathway, suggesting that Nb cells may be susceptible to exogenous stresses.<sup>26</sup> Because *TFAP2B* is involved in other cancers,<sup>27</sup> it may contribute to high aggressiveness neuroblastoma. NTs-SP also express *TOP2A*, a gene located in the 17q12-q22 region that is frequently gained and translocated in neuroblastoma.<sup>28-30</sup> *TOP2A* protein is associated with resistance to cytotoxic drugs.<sup>31</sup> We showed that *TOP2A* is expressed in malignant neuroblasts of NTs-SP, supporting the usefulness of topotecan as drug currently used in the treatment of neuroblastomas.<sup>32</sup> Eight genes (*BIRC5*, *CDH10*, *CENPF*, *DES*, *MLF1IP*, *MYCN*, *RRM2*, *TOP2A*) expressed in NTs-SP were also found highly transcribed in normal neuroblasts of human fetal adrenal glands.<sup>4</sup> The expression of these genes in NTs-SP suggests an early block of differentiation of neuroblastic elements.

Gene ontology analysis indicates that genes associated with signal transduction, cell differentiation, and proapoptotic pathways are highly expressed in NTs-SR. Moreover, these tumors show high expression of *MAL*, a caspase-activating protease gene,<sup>33</sup> *EGR3*, an early gene induced in cells committed to apoptosis,<sup>34</sup> and *CLU*, a gene involved in proapoptotic

mechanisms.<sup>35</sup> NTs-SR also express *PLP1*, a target of *SOX10*, which has recently been reported more expressed in ganglioneuromas than in neuroblastomas.<sup>36</sup>

Sixteen genes were differently expressed between NT-SP and NT-SR categories by the SAM and GT combined approach. Five genes up-regulated in NTs-SP encode for transcriptional factors (*CENPE*, *EYA1*, *PBK*, *TOP2A*, *TFAP2B*), whereas only 1 of 11 highly expressed genes in NTs-SR encodes for a nuclear factor (*NR4A2*). The *NR4A2* expression in NTs-SR suggests a putative role of this transcription factor in stroma tumor, and functional studies are ongoing on its activity in SS cells. The other 10 genes overexpressed in NTs-SR are involved in lipid metabolism and electron transport pathways. Only 3 of 16 genes (*TFAP2B* in NTs-SP and *GPM6B*, *MAL* in NTs-SR) are related to nervous system development.

In conclusion, we demonstrated that Nb and SS cell-specific signatures differ for a set of genes that are involved in distinct pathways. In particular, we observed that Nb cells highly express genes involved in inhibition of apoptosis, cell cycle, and DNA repair pathways. Our analysis showed low intratumoral heterogeneity at the mRNA level in both NTs-SP and NTs-SR. Interestingly, we observed that Nb cells embedded in SS cells are characterized by a “stroma-rich” gene signature. This finding suggests that the tumor microenvironment may modify the gene expression of Nb cells, supporting the hypothesis of paracrine activity of SS *vs* Nb cells. Present results should be taken into account to improve the classification of aggressive tumors and for new targeting therapy.

## REFERENCES

- Shimada H, Ambros IM, Dehner LP, Hata J, Joshi VV, Roald B. Terminology and morphologic criteria of neuroblastic tumors: recommendations by the International Neuroblastoma Pathology Committee. *Cancer*. 1999;86:349-363.
- Takita J, Ishii M, Tsutsumi S, et al. Gene expression profiling and identification of novel prognostic marker genes in neuroblastoma. *Genes Chromosomes Cancer*. 2004;40:120-132.
- Wei JS, Greer BT, Westermann F, et al. Prediction of clinical outcome using gene expression profiling and artificial neural networks for patients with neuroblastoma. *Cancer Res*. 2004;64:6883-6891.
- De Preter K, Vandesompele J, Heimann P, et al. Human fetal neuroblast and neuroblastoma transcriptome analysis confirms neuroblast origin and highlights neuroblastoma candidate genes. *Genome Biol*. 2006;7:R84.
- Ohira M, Morohashi A, Inuzuka H, et al. Expression profiling and characterization of 4200 genes cloned from primary neuroblastomas: identification of 305 genes differentially expressed between favourable and unfavourable subsets. *Oncogene*. 2003;22:5525-5536.
- Oberthuer A, Berthold F, Warnat P, et al. Customized oligonucleotide microarray gene expression-based classification of neuroblastoma patients outperforms current clinical risk stratification. *J Clin Oncol*. 2006;24:5070-5078.
- Coco S, Defferrari R, Scaruffi P, et al. Genome analysis and gene expression profiling of neuroblastoma and ganglioneuroblastoma reveal differences between neuroblastic and Schwannian stromal cells. *J Pathol*. 2005;207:346-357.
- Tusher VG, Tibshirani R, Chu G. Significance analysis of microarrays applied to the ionizing radiation response. *Proc Natl Acad Sci U S A*. 2001;98:5116-5121.
- von Neumann J, Morgenstern O. Theory of games and economic behaviour. Princeton, NJ: Princeton University Press; 1944.
- Shapley LS: A value for n-person games. In: Kuhn W, Tucker AW, eds. Contributions to the theory of games II. New York, NY: Princeton University Press; 1953:307-317.
- Moretti S, Patrone F, Bonassi S. The class of microarray games and the relevance index for genes. *Top*. 2007;15:256-280.
- Pasanen T, Saarela J, Saarikko I, et al. DNA microarray data analysis. Espoo, Finland: CSC Scientific Computing Ltd; 2003:100-102.
- Brodeur GM, Pritchard J, Berthold F, et al. Revision of the international criteria for neuroblastoma diagnosis, staging and response to treatment. *J Clin Oncol*. 1993;11:1466-1477.
- Simon RM, Korn EL, McShane LM, Radmacher MD, Wright GW, Zhao Y. Design And Analysis Of DNA Microarray Investigations. New York, NY: Springer; 2003.
- Gautier L, Cope L, Bolstad BM, Irizarry RA. affy—analysis of Affymetrix GeneChip data at the probe level. *Bioinformatics*. 2004;20:307-315.
- Huber W, von Heydebreck A, Sultmann H, Poustka A, Vingron M. Variance stabilization applied to microarray data calibration and to the quantification of differential expression. *Bioinformatics*. 2002;18(suppl 1):S96-S104.
- Gautier L, Moller M, Friis-Hansen L, Knudsen S. Alternative mapping of probes to genes for Affymetrix chips. *BMC Bioinformatics*. 2004;5:111-118.
- Storey JD, Tibshirani R. SAM thresholding and false discovery rates for detecting differential gene expression in DNA microarray. In: Parmigiani G, Garrett ES, Irizarry RA, Zeger SL, eds. The Analysis Of Gene Expression Data: Methods And Software. New York, NY: Springer; 2003.
- Benjamini Y, Hochberg Y. Controlling the false discovery rate: a practical and powerful approach to multiple testing. *J R Stat Soc*. 1995;57:289-300.
- Soric B. Statistical discoveries and effect-size estimation. *J Am Stat Assoc*. 1989;84:608-610.
- Hiyama E, Hiyama K, Yamaoka H, Sueda T, Reynolds CP, Yokoyama T. Expression profiling of favourable and unfavourable neuroblastomas. *Pediatr Surg Int*. 2004;20:33-38.
- Krasnoselsky AL, Whiteford CC, Wei JS, et al. Altered expression of cell cycle genes distinguishes aggressive neuroblastoma. *Oncogene*. 2005;24:1533-1541.
- McArdle L, McDermott M, Purcell R, et al. Oligonucleotide microarray analysis of gene expression in neuroblastoma displaying loss of chromosome 11q. *Carcinogenesis*. 2004; 25:1599-1609.
- Islam A, Kageyama H, Takada N, et al. High expression of Survivin, mapped to 17q25, is significantly associated with poor prognostic factors and promotes cell survival in human neuroblastoma. *Oncogene*. 2000;19:617-623.

25. Ito R, Asami S, Motohashi S, et al. Significance of survivin mRNA expression in prognosis of neuroblastoma. *Biol Pharm Bull.* 2005;28:565-568.
26. Pearson G, Robinson F, Beers Gibson T, et al. Mitogen-activated protein (MAP) kinase pathways: regulation and physiological functions. *Endocr Rev.* 2001;22:153-183.
27. Eckert D, Buhl S, Weber S, Jager R, Schorle H. The AP-2 family of transcription factors. *Genome Biol.* 2005;6:246-253.
28. Cunsolo CL, Bicocchi MP, Petti AR, Tonini GP. Numerical and structural aberrations in advanced neuroblastoma tumors by CGH analysis; survival correlates with chromosome 17 status. *Br J Cancer.* 2000;83:1295-1300.
29. Yoon KJ, Danks MK, Ragsdale ST, Valentine MB, Valentine VA. Translocations of 17q21 approximately qter in neuroblastoma cell lines infrequently include the topoisomerase IIalpha gene. *Cancer Genet Cytogenet.* 2006;167:92-94.
30. Lastowska M, Van Roy N, Bown N, et al. Molecular cytogenetic delineation of 17q translocation breakpoints in neuroblastoma cell lines. *Genes Chromosomes Cancer.* 1998;23:116-122.
31. Gyorfy B, Serra V, Jurchott K, et al. Prediction of doxorubicin sensitivity in breast tumors based on gene expression profiles of drug-resistant cell lines correlates with patient survival. *Oncogene.* 2005;24:7542-7551.
32. Simon T, Langer A, Berthold F, Klingebiel T, Hero B. Topotecan and etoposide in the treatment of relapsed high-risk neuroblastoma: results of a phase 2 trial. *J Pediatr Hematol Oncol.* 2007;29:101-106.
33. Kohler C, Hakansson A, Svanborg C, Orrenius S, Zhivotovsky B. Protease activation in apoptosis induced by MAL. *Exp Cell Res.* 1999;249:260-268.
34. Kokkinakis DM, Brickner AG, Kirkwood JM, et al. Mitotic arrest, apoptosis, and sensitization to chemotherapy of melanomas by methionine deprivation stress. *Mol Cancer Res.* 2006;4:575-589.
35. Shannan B, Seifert M, Boothman DA, Tilgen W, Reichrath J. Clusterin and DNA repair: a new function in cancer for a key player in apoptosis and cell cycle control. *J Mol Histol.* 2006;37:183-188.
36. Gershon TR, Oppenheimer O, Chin SS, Gerald WL. Temporally regulated neural crest transcription factors distinguish neuroectodermal tumors of various malignancy and differentiation. *Neoplasia.* 2005;7:575-584.